Available online at www.sciencedirect.com
SCIENCE DIRECT®
Geochimica et Cosmochimica Acta 70 (2006) 595–607
Geochimica
www.elsevier.com/locate/gca

Citrate impairs the micropore diffusion of phosphate into pure and C-coated goethite

Christian Mikutta *, Friederike Lang, Martin Kaupenjohann

Department of Soil Science, Institute of Ecology, Berlin University of Technology, Salzufer 12, D-10587 Berlin, Germany

Received 27 June 2005; accepted in revised form 13 October 2005

Abstract

Anions of polycarboxylic low-molecular-weight organic acids (LMWOA) compete with phosphate for sorption sites of hydrous Fe and Al oxides. To test whether the sorption of LMWOA anions decreases the accessibility of micropores (<2 nm) of goethite (α-FeOOH) for phosphate, we studied the kinetics of citrate-induced changes in microporosity and the phosphate sorption kinetics of synthetic goethite in the presence and absence of citrate in batch systems for 3 weeks (500 μM of each ion, pH 5). We also used C-coated goethite obtained after sorption of dissolved organic matter in order to simulate organic coatings in the soil. We analyzed our samples with N_2 adsorption and electrophoretic mobility measurements. Citrate clogged the micropores of both adsorbents by up to 13% within 1 h of contact. The micropore volume decreased with increasing concentration and residence time of citrate. In the absence of citrate, phosphate diffused into micropores of the pure and C-coated goethite. The C coating (5.6 μmol C m^{-2}) did not impair the intraparticle diffusion of phosphate. In the presence of citrate, the diffusion of phosphate into the micropores of both adsorbents was strongly impaired. We attribute this to the micropore clogging and the ligand-induced dissolution of goethite by citrate. While the diffusion limitation of phosphate by citrate was stronger when citrate was added before phosphate to pure goethite, the order of addition of both ions to C-coated goethite had only a minor effect on the intraparticle diffusion of phosphate. Micropore clogging and dissolution of microporous hydrous Fe and Al oxides may be regarded as potential strategies of plants to cope with phosphate deficiency in addition to ligand-exchange.

1. Introduction

Phosphate sorption to hydrous Fe oxides comprises a rapid initial adsorption to external surfaces followed by a slow reaction, which can last for days or weeks (Barrow et al., 1981; Torrent et al., 1990). The slow phosphate immobilization has been attributed to the diffusion of phosphate into microporous imperfections of the crystals, micro- and mesopores located between the crystal domains (Torrent, 1991; Strauss, 1992; Barrow et al., 1993; Fischer et al., 1996; Strauss et al., 1997; Makris et al., 2004), or the diffusion into aggregates of particles (Anderson et al., 1985; Willet et al., 1988). Torrent et al. (1990, 1992) observed that a portion of phosphate sorbed to microporous Fe oxides was not desorbable in 0.1 M KOH. This finding was attributed to both the slow rediffusion of phosphate out of micropores and the formation of binuclear surface complexes of phosphate. Also, Fuller et al. (1993) showed that the rate of the slow sorption of arsenate to ferrihydrite was limited by intraparticle diffusion.

Polycarboxylic low-molecular-weight organic acids (LMWOA) successfully compete with phosphate for sorption sites (Violante et al., 1991; Bhatti et al., 1998; Geelhoed et al., 1998). This is especially relevant for the soil rhizosphere where exudation of LMWOA anions by plants and microorganisms is high. When polycarboxylic LMWOA anions are added to Al and Fe oxides or soils before phosphate, a decrease in phosphate sorption is generally noticed (Hue, 1991; Violante et al., 1991; Geelhoed et al., 1998; Hu et al., 2001). This may be attributed to direct site blocking, electrostatic repulsion or diffusion of

* Corresponding author. Fax: +49 30 314 73 548.
E-mail address: christian.mikutta@tu-berlin.de (C. Mikutta).

0016-7037/$ - see front matter © 2005 Elsevier Inc. All rights reserved.
doi:10.1016/j.gca.2005.10.032

LMWOA anions into small nm-pores of the adsorbent, which may result in a steric and/or electrostatic diffusion impedance for phosphate ions. Considering the volume of anhydrous citric acid (0.775 nm^3, Nordman et al., 1960), a decreased accessibility of micropores (<2 nm) to phosphate due to the sorption of citrate in micropores can be expected. Here, we hypothesized that citrate clogs the micropores of goethite, thus reducing the diffusion of phosphate into the adsorbent.

In the soil environments, microbes rapidly consume LMWOA anions, causing average half lives of LMWOA anions in the soil solution to be fairly low. For example, Jones and Darrah (1994) and Jones (1998) reported half lives of less than 12 h for citrate. If our proposed mechanism was relevant in vivo, the micropore clogging of hydrous Fe oxides by citrate should proceed within hours. Therefore, we tested the micropore clogging kinetics of pure and C-coated goethite by citrate within up to 12 h.

In soils and sediments clean oxide surfaces seldom exist as they are partly coated with organic matter (Mayer, 1999; Mayer and Xing, 2001; Gerin et al., 2003). Coatings created by dissolved organic matter (DOM) and polygalacturonate (PGA) have been shown to clog micropores of hydrous Fe and Al oxides (Lang and Kaupenjohann, 2003; Kaiser and Guggenberger, 2003; Mikutta et al., 2004). The micropore clogging of goethite by polygalacturonate at a low surface loading (6.3 μmol C m^{-2}) has been shown to decrease the slow phosphate sorption, i.e., the diffusion of phosphate into intraparticle pores of goethite (Mikutta et al., 2006).

The presence of C-coatings at the surface of pedogenic hydrous Fe oxides may change the effect of LMWOA anions in different ways: low-molecular-weight organic acids may exchange for pre-sorbed macromolecular natural organic matter by sorption competition, or be able to disrupt organo-mineral associations either by complexation of bridging multivalent cations (Edwards and Bremmer, 1967) or by dispersion (Pinheiro-Dick and Schwertmann, 1996). These processes may liberate diffusion pathways for phosphate, thus enhancing the slow, continuous and strong phosphate fixation in intraparticle pores. Alternatively, LMWOA anions may further increase the micropore clogging already induced by the sorption of high-molecular weight compounds, thereby impairing the diffusion of phosphate into micropores. For this reason, we studied the phosphate immobilization kinetics of pure and C-coated goethite in the presence and absence of citrate for 3 weeks. In addition, the changes in specific surface area (SSA), nanoporosity, and electrophoretic mobility of pure and C-coated goethite upon sorption of phosphate and/or citrate were also analyzed. All experiments were conducted at pH 5 in order to resemble pH conditions of the soil rhizosphere and the bulk of acid soils. At conditions where the pH of soil solution is lower than the isoelectric point of hydrous Fe and Al oxides ($pH < pH_{iep}$), the availability of phosphate to plants is strongly reduced because of its sorption to positively charged hydrous Fe and Al oxide surfaces. In addition, goethite dissolution by protonation and the influence of dissolved CO_2 should be kept to a minimum in the sorption experiments.

2. Materials and methods

2.1. Preparation and characterization of the adsorbents

Goethite was synthesized in one batch by oxidative hydrolysis of Fe(II) ($FeSO_4 \cdot 7H_2O$, Merck, extra pure) at pH 7 using H_2O_2 as an oxidant. The precipitate was washed until the electric conductivity was below 10 μS cm^{-1}, freeze-dried, softly ground and sieved to a particle size <200 μm. Powder X-ray diffraction analysis (Siemens D5005, CuKα radiation) showed typical reflections of goethite without any detectable contamination. The goethite was analyzed with transmission electron microscopy (JEOL JSEM 200B). Transmission electron microscopy images showed a broad size distribution of crystallites due to differing rates of Fe(II) oxidation during synthesis. Larger acicular crystallites are accompanied by smaller ones having no particular habit (Fig. 1). The acid–ammonium oxalate-soluble Fe content (Blakemore et al., 1987) of the goethite was 4.9 wt%. The acid–ammonium oxalate-soluble Fe is usually ascribed to Fe contained in amorphous or poorly crystalline Fe minerals (e.g., Olson and Ellis, 1982). However, there is evidence that this treatment will also dissolve crystalline Fe oxides (McKeague et al., 1971; Schwertmann, 1973; Walker, 1983; Borggaard, 1988, 1990; Fine and Singer, 1989). Hence, an acid–ammonium oxalate-soluble Fe content of ~5 wt% indicates that the content in residual ferrihydrite is low in our goethite sample. Possible effects of residual ferrihydrite on porosity changes induced by phosphate/citrate are accounted for in Section 3. The isoelectric point, pH_{iep}, of the goethite used was 7.6 as determined by potentiometric titration of the goethite in 0.01 M KNO_3 solution (~0.01 g L^{-1} goethite)

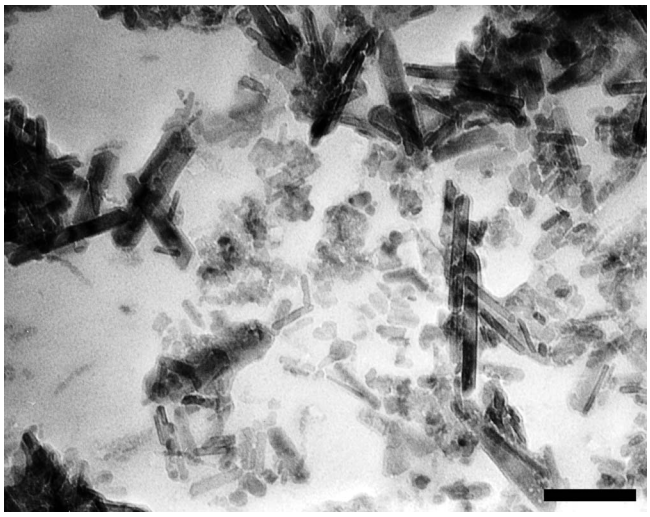

Fig. 1. Transmission electron micrograph of the goethite used in this study (102,000×). The bar indicates 100 nm.

using a MPT-1 autotitrator connected with a Zetasizer 2000 (Malvern Instruments, UK). The density of goethite was found to be 4.2 ± 0.1 g cm^{-3} as determined with a Quantachrome He-pycnometer.

To simulate organic coatings of the mineral, the goethite was coated with dissolved organic matter. The DOM solution was obtained from an aqueous extract of a forest-floor soil sample of an O-horizon of a Haplorthod. The forest-floor material was extracted in doubly deionized water for 20 h at pH 5 (1:6 w/v). The extract was membrane-filtered (0.45 μm) and analyzed for total organic C (TOC) using a Shimadzu TOC-5050A Autoanalyzer. The TOC concentration was 220.1 ± 4.9 mg C L^{-1}. The average size of colloids in the DOM filtrate was 191 ± 18 nm as measured by dynamic light scattering (Malvern HPPS, UK). Phosphate in the DOM solution was measured photometrically at 710 nm using the method of Murphy and Riley (1962) after ultracentrifugation at 440,000*g* for 1 h. The phosphate concentration found would led to a maximal possible preloading of ~0.08 μmol P m^{-2} when goethite was coated with DOM, which is low compared to the maximal sorption capacity of goethite of 2.5 μmol P m^{-2} (Torrent et al., 1990). Multivalent cations in the DOM extract were determined with atomic absorption spectrometry (Perkin-Elmer 1100B). The amount of charge equivalents in the DOM extract was 71 μmol_c L^{-1} Ca, 11 μmol_c L^{-1} Mg, and 33 μmol_c L^{-1} Fe.

Prior to sorption of DOM to goethite, the hydrous Fe oxide was ultrasonicated for 30 min and hydrated in doubly deionized water for 48 h in a glass volumetric flask in order to hydrate adsorption sites (2:25 w/v). The pH of the stock suspension was adjusted to 5.0 ± 0.02 with diluted HNO_3. Goethite was reacted with DOM solution (179.5 mg C L^{-1}) in the dark (1:100 w/v, pH 5 ± 0.2) under magnetic stirring in a 2-L PE bottle. After 24 h, the suspension was membrane-filtered (0.45 μm). The filter residue was washed with 2.5 L doubly deionized water adjusted to pH 5 with dilute HNO_3 or KOH to remove excess DOM-C and freeze-dried. The C content of the goethite was 12.1 mg g^{-1} as determined with a Carlo Erba C/N NA 1500 N Analyzer. The C-coated goethite was stored in the dark until use.

2.2. Analysis of porosity changes induced by citrate

Citrate was used in the sodium form $C_6H_5Na_3O_7 \cdot 2H_2O$ (Merck, p.a.). The effect of citrate on the accessibility of the micropores was studied at different citrate concentrations for C-coated goethite only and different contact times for both adsorbents.

Citric acid concentrations in the soil solution are typically less than 370 μM (Jones, 1998 and references therein). Hence, for studying the concentration effect of citrate, the C-coated goethite (2 g L^{-1}) was reacted with solutions containing 20, 100 and 300 μM citrate in a 2-L PE bottles at pH 5 on a reciprocating shaker at 130 rev min^{-1}. Potassium nitrate (0.01 M) was used as background electrolyte. At pH 5, the dominating citrate species are H_2Cit^- (28.3%) and $HCit^{2-}$ (66.9%). Since the average half life of citrate in soils is 2–3 h (Jones, 1998) or larger (11.7 h; Jones and Darrah, 1994), we chose a contact time of 3 h. After 3 h, the suspensions were filtered (0.45 μm), washed with 1 L 0.01 M KNO_3 solution (pH 5), freeze-dried, softly ground to <200-μm particle size and further analyzed by N_2 adsorption.

The influence of residence time of citrate on nanoporosity of pure and C-coated goethite was tested at a citrate concentration of 300 μM in 0.01 M KNO_3 solution (pH 5) with a solid concentration of 1 g L^{-1}. The suspensions were reacted on a reciprocating shaker at 130 rev min^{-1}. After 1, 6 and 12 h, the suspensions were membrane-filtered (0.45 μm), the filter residues were washed with 1 L 0.01 M KNO_3 solution (pH 5), freeze-dried, and stored in glass bottles at 278 K. The freeze-dried filter residues were further analyzed by N_2 adsorption after soft grinding to <200-μm particle size.

In both experiments, the reaction vessels were coated with Al-foil in order to inhibit the photochemical dissolution of goethite in the presence of citrate. The pH was manually maintained with dilute HNO_3 or KOH at pH 5 ± 0.2. Citrate, TOC and Fe were measured in the 0.45-μm filtrates. The citrate concentration was determined photometrically at 340 nm by measuring the stoichiometric decrease in nicotinamide–adenine dinucleotide (NADH) concentration in an enzymatic reaction with a Speccord 200 photometer (Analytik Jena AG) (Möllering and Gruber, 1966). The detection limit of the method is 2.6 μM citric acid and linearity of the determination ranges from 2.6 to 2.08×10^3 μM citric acid (Boehringer–Mannheim/R-Biofarm, Germany). Matrix interferences with dissolved Fe did not occur. Additionally, the amount of citrate-C sorbed onto pure goethite was measured with an Elementar Vario EIII C/N/S Analyzer. Iron was analyzed with graphite furnace AAS (Perkin-Elmer AAnalyst 700). All experiments were conducted in triplicate.

2.3. Phosphate sorption kinetics in the absence and presence of citrate

Phosphate sorption onto pure and C-coated goethite was measured for 3 weeks in batch experiments in a temperature-controlled room at 298 K. Reaction vessels were coated with Al foil and 100 μL of 0.05 M $AgNO_3$ was added to inhibit microbial activity. Phosphate was used as KH_2PO_4 (Merck, p.a.). The solid concentration was 0.5 g L^{-1} in 0.01 M KNO_3 and the pH was manually maintained at 5 ± 0.2 using dilute HNO_3 or KOH. At pH 5, the predominant species of phosphate is $H_2PO_4^-$. To hydrate adsorption sites and disperse particles, 200 mL of background electrolyte (pH 5) was given to 0.6 g adsorbent. The samples were then shaken on a horizontal shaker at 100 rev min^{-1} for 3 h. Then 1 L of 600 μM phosphate solution in 0.01 M KNO_3 (pH 5) was added to get a final phosphate concentration of 500 μM. The pH was readjusted to

5 with dilute HNO_3 or KOH. Samples were shaken on a rotary shaker at 10 rev min^{-1}. After 0.5, 1, 2, 4, 8, 24, 48, 168, 336, and 504 h, a 10-mL aliquot was removed and 0.45-μm membrane-filtered. An ultracentrifuged (1 h at 440,000*g*) sub-sample of the 0.45-μm filtrate was analyzed for phosphate and Fe. Additionally, total organic C was measured in the 0.45-μm filtrate (Shimadzu TOC-5050A Autoanalyzer). We ensured that sampling did not result in a relative enrichment of the adsorbent in the reaction vessels. The solid concentrations of the sub-samples varied by less than 5 wt%. The 0.45-μm filter residue was washed with 40 mL doubly deionized water and freeze-dried for N_2 adsorption and electrophoretic mobility measurements. The 0.45-μm filtrates were stored at −18 °C until they were defrosted for electrophoretic mobility measurements.

The influence of citrate on the kinetics of phosphate sorption to pure and C-coated goethite was studied at equimolar ion concentrations of 500 μM. In one experiment, phosphate and citrate were added simultaneously '(C + P)'. After equilibration of goethite and C-coated goethite in the background electrolyte as described above, 1 L of 0.01 M KNO_3 solution containing equimolar amounts of phosphate and citrate (600 μM) was added to obtain a concentration of 500 μM of each ion. Phosphate sorption was again monitored over 3 weeks.

In a second experiment, citrate was added before phosphate 'C + P'. Six hundred milligrams of pure and C-coated goethite was equilibrated in 1.2 L of 0.01 M KNO_3 solution (pH 5) containing 500 μM citrate. After 3 h, the solution was spiked with 10 mL phosphate solution to give a phosphate concentration of 500 μM and analyzed for phosphate, Fe and citrate as described above. All sorption experiments were performed in triplicate.

In all experiments, concentrations expressed on a unit mass or surface area basis were corrected for the water content in pure and C-coated samples. The water content was determined by outgassing the sample in a Quantachrome Autosorb-1 automated gas sorption system (Quantachrome, Syosset, NY) at room temperature until the pressure increase rate by vapor evolution was below about 1.3 Pa min^{-1} within a 0.5-min test interval. This was done in order to avoid phase transformations and the loss of structural water. The water content of both microporous adsorbents was 17 wt%.

2.4. Phosphate sorption data interpretation

We combined a modified first-order rate equation with the parabolic rate law (Crank, 1976) in order to account for the fast and the slow sorption of phosphate to goethite, respectively (Lang and Kaupenjohann, 2003):

$$q_t = c_m - a_0\ e^{-kt} + bt^{0.5}, \quad (1)$$

where q_t is the amount of phosphate sorbed at time t (μmol m^{-2}), c_m is the maximum amount of phosphate sorbed by the fast reaction (μmol m^{-2}) and represents the portion of phosphate that is sorbed to external goethite surfaces, $c_m - a_0$ is the amount of phosphate sorbed instantaneously (faster than could be quantified by the batch approach, μmol m^{-2}), k is the rate constant of the initial fast phosphate sorption (h^{-1}), t is time (h), and b is the apparent rate constant of the slow sorption (μmol m^{-2} $h^{-0.5}$).

The rate constant of the slow phosphate sorption, b, is related to the apparent diffusion constant $(D/r^2)_{app}$ (h^{-1}):

$$b = 4q_\infty \pi^{-0.5} (D/r^2)_{app}^{0.5}, \quad (2)$$

where q_∞ is the amount of phosphate diffused at infinite time, D is the apparent diffusion coefficient (m^2 h^{-1}), and r is the radius of diffusion (m). To obtain parameters c_m, a_0, k and b, Eq. (1) was fitted to our phosphate sorption data using SigmaPlot for Windows (SPSS). We used the total amount of phosphate present at $t = 0$ corrected for the total amount of phosphate sorbed to external surfaces (c_m) as an approximation for q_∞ in Eq. (2) to calculate the apparent diffusion constant $(D/r^2)_{app}$. The amount of phosphate sorbed by the slow reaction was approximated by

$$P_{slowly} = q_{504h} - c_m, \quad (3)$$

where q_{504h} is the amount of phosphate sorbed after 504 h (μmol m^{-2}) and c_m is the total amount of phosphate sorbed by the fast phosphate reaction.

2.5. Surface area and porosity measurements

Specific surface area and pore volume were determined with a Quantachrome Autosorb-1 automated gas sorption system (Quantachrome, Syosset, NY) using N_2 as an adsorbate. Approximately, 80 mg of sample was degassed until the pressure increase rate by vapor evolution was below about 1.3 Pa min^{-1} within a 0.5-min test interval. Helium was used as a backfill gas. We used 71-point N_2 adsorption and desorption isotherms from 1.0×10^{-5} to 0.995 P/P_0. Specific surface area was calculated from the BET equation (Brunauer et al., 1938).

Micropore (<2 nm) porosity and average micropore diameter were determined according to the Dubinin–Radushkevic method (DR method; Gregg and Sing, 1982). The mesopore size distribution (2–50 nm) was calculated on the desorption leg using the BJH method (Barrett et al., 1951). Separation between small (2–5 nm), medium (5–10 nm) and large mesopores (10–50 nm) was achieved by linear interpolation of BJH desorption data. Total pore volume was taken at 0.995 P/P_0 and the average pore diameter was calculated as

$$D_p = 4V_{liq}/SSA, \quad (4)$$

where V_{liq} is the volume of liquid N_2 contained in the pores at 0.995 P/P_0 and SSA is the BET surface area. All isotherms were recorded in triplicate.

2.6. Electrophoretic mobility measurements

The electrophoretic mobility, μ, was monitored over the entire phosphate/citrate sorption run. After each reaction

time, about 200 μg of freeze-dried 0.45-μm filter residue was resuspended into 4 mL of phosphate/citrate solution obtained after 0.45-μm membrane filtration of the goethite suspension.

To facilitate sample handling, we used dried solids that were stored in the dark at ambient relative humidity (~30%) for electrophoretic mobility measurements. Preliminary tests revealed that during phosphate sorption for 1 week, electrophoretic mobilities of pure and C-coated goethite in aqueous suspensions (0.01 M KNO_3, pH 5) did not significantly differ from those obtained from samples that were freeze-dried after 0.45-μm membrane filtration and resuspended in background electrolyte for electrophoretic measurements (*t*-test, $P < 0.05$).

The electrophoretic mobility was determined at 298 K with a Zetasizer 2000 (Malvern Instruments, UK). Before the measurements, the instrument was calibrated with a ζ-potential transfer reference, which is referenced to the NIST goethite standard SRM1980 (Malvern Instruments, UK). Ten measurements were performed within less than 8 min and the average value was recorded. The ζ-potential was calculated from the electrophoretic mobility using the Smoluchowski equation (Hunter, 1981):

$$\mu = \varepsilon_0 D\zeta/\eta, \quad (5)$$

where ε_0 is the permittivity of vacuum, D is the dielectric constant of water, ζ is the ζ-potential and η is the coefficient of viscosity. It is generally assumed that the ζ-potential represents the potential at a shear plane located in the diffuse layer close to the Stern layer (Hunter, 1981).

3. Results and discussion

3.1. Pore clogging of goethite by DOM and citrate

Sorption of DOM to goethite led to a significant decrease in the volume of micropores and small mesopores <10 nm (Table 1). Similar results have been obtained by several researchers (Lang and Kaupenjohann, 2003; Kaiser and Guggenberger, 2003; Mikutta et al., 2004). In contrast, the average micropore diameter was not affected by the DOM treatment. This observation might be explained in

Table 1
Concentration and residence time effects of citrate on meso- and microporosity of pure and C-coated goethite at pH 5

Treatment	Mesopore volume ($mm^3\ g^{-1}$)			Micropore volume ($mm^3\ g^{-1}$)	Average micropore diameter (nm)
	2–5 nm	5–10 nm	10–50 nm		
Citrate concentration[a]					
Goethite-initial[b]	75 (6)a	89 (3)a	420 (12)a	57 (1)a	0.87 (0.01)a
Goethite/DOM-initial[b]	53 (5)b	76 (2)b	417 (9)a	44 (0)b	0.87 (0.01)a
Goethite/DOM + 20 μM citrate	48 (3)b	78 (4)b	401 (7)ab	42 (0)c	0.85 (0.01)ab
Goethite/DOM + 100 μM citrate	46 (2)b	76 (3)b	395 (13)a	40 (0)d	0.84 (0.00)bc
Goethite/DOM + 300 μM citrate	45 (0)b	79 (4)b	393 (9)b	37 (1)e	0.82 (0.01)d
Citrate residence time[c]					
Goethite control					
1 h	62 (4)	82 (1)	359 (2)	53 (1)	0.88 (0.01)
6 h	61 (2)	82 (0)	342 (4)	52 (0)	0.87 (0.02)
12 h	58 (1)	79 (1)	345 (13)	51 (1)	0.88 (0.01)
Goethite + citrate					
1 h	58 (4)NS	80 (3)NS	361 (4)NS	46 (0)***	0.83 (0.00)**
6 h	56 (3)NS	83 (3)NS	356 (5)*	44 (0)***	0.82 (0.01)*
12 h	53 (3)*	80 (3)NS	360 (3)NS	42 (0)***	0.81 (0.01)***
Goethite/DOM control					
1 h	46 (27)	77 (2)	387 (6)	41 (0)	0.86 (0.01)
6 h	49 (3)	77 (3)	374 (5)	42 (1)	0.87 (0.01)
12 h	48 (3)	75 (2)	383 (1)	43 (0)	0.87 (0.00)
Goethite/DOM + citrate					
1 h	47 (4)NS	76 (3)NS	369 (3)**	38 (0)***	0.83 (0.00)**
6 h	45 (3)NS	78 (3)NS	373 (6)NS	37 (0)***	0.83 (0.01)**
12 h	51 (4)NS	80 (2)*	355 (8)**	37 (0)***	0.82 (0.00)***

Goethite-initial and Goethite/DOM-initial give the goethite properties at the beginning of the sorption experiments, i.e., no solution contact.
Means were compared with the unpaired *t*-test. Values in the same column that are followed by the same letter are not statistically different at $P < 0.05$. Values are given as means ± SD. In the citrate residence time experiment, means of each residence time were compared (+citrate versus respective control treatment).
NS indicates nonsignificance at $P = 0.05$.
*,**,*** Significant at the 0.05, 0.01, and 0.001 probability level, respectively.
[a] Three hours contact time, 2 g L^{-1} solid concentration, and $I = 0.01$ M KNO_3.
[b] Initial, no solution contact.
[c] 300 μM citrate addition, 1 g L^{-1} solid concentration, and $I = 0.01$ M KNO_3.

two ways: (1) DOM sorption might cause a complete clogging of some micropores for N_2 at 77 K, while other micropores remained free of any organic matter, or (2) DOM treatment might induce an occlusion of mineral surfaces upon drying. Mayer and Xing (2001) demonstrated for acid soils that a large portion of mineral surface area is occluded by organic matter.

The amount of citrate sorbed onto pure and C-coated goethite after 12 h at pH 5 was 1.7 and 1.6 μmol m^{-2}, respectively, which is close to the reported maximum level of citrate sorption onto goethite with 1.9 μmol m^{-2} (Cornell and Schindler, 1980). Citrate sorption to both adsorbents resulted in a pronounced decrease in the micropore volume and the average micropore diameter (Table 1). The effect increased with increasing contact time of citrate and, in the case of C-coated goethite, increased with increasing citrate concentration (Table 1). The results indicate a micropore clogging by citrate within less than 1 h of citrate sorption. Absolute changes in micropore volumes upon sorption of citrate were highly significant but about as small as changes reported for hydrous Fe and Al oxides of drinking-water treatment residuals after sorption of phosphate for 80 days (Makris et al., 2004).

The miropore volumes of pure goethite decreased in the background electrolyte, even without the addition of DOM or citrate (see 'Goethite control', Table 1). However, the decrease in micropore volume was significantly larger in the citrate treatments (Table 1).

Ligand-promoted dissolution of goethite can be ruled out as a course for the porosity changes detected in the presence of citrate, as Fe concentrations determined in solution were small, e.g., the addition of 300 μM citrate to C-coated goethite for 3 h resulted in a goethite dissolution of only 0.3 mol% Fe. Taking an average N_2-BET surface area of 242 $m^2\,g^{-1}$ of 10 synthetic 2-line and 6-line ferrihydrites (Liang et al., 2000; Cornell and Schwertmann, 2003, Table 5.1, p.106), and assuming (i) a molecular weight of ferrihydrite of 480 g mol^{-1} ($Fe_5HO_8 \cdot 4H_2O$, Towe and Bradley, 1967) and (ii) that all acid–ammonium oxalate-soluble Fe (4.9 wt%) comes from residual ferrihydrite still present in our solid, a simple alligation calculation shows that maximal 6 $m^2\,g^{-1}$ solid could be attributed to residual ferrihydrite. The decrease in the DR-micropore surface area after sorption of citrate to pure and C-coated goethites for 12 h was 23 and 16 $m^2\,g^{-1}$, respectively. Therefore, we take the statistically significant decreases in micropore volumes and micropore diameters obtained from applying the DR model to the N_2 adsorption data of citrate-treated goethites as direct evidence for pore clogging by citrate. It should be noted that these micropore diameters are average diameters. From a chemical standpoint, the tiny decreases observed (<0.1 nm, Table 1) suggest that no monolayer sorption by citrate in micropores occurred.

Our results show that the sorption of citrate in micropores is a fast process being detectable by N_2 adsorption just 1 h after citrate addition to both adsorbents.

3.2. Phosphate sorption kinetics in the absence of citrate

Pure and C-coated goethite sorbed 2.1 and 1.8 μmol P m^{-2}, respectively. The value for pure goethite is smaller than the 2.5 μmol P m^{-2} that are maximal expected to sorb on a (1 0 1) goethite surface with two singly coordinated surface hydroxyls per 0.68 nm^2 at a maximum loading (Torrent et al., 1990; Cornell and Schwertmann, 2003). Sorption of phosphate to pure and C-coated goethite did not reach an equilibrium within 3 weeks and showed a biphasic pattern (Fig. 2), which is commonly observed for phosphate sorption to soils and hydrous Fe oxides (Torrent, 1987; Barrow et al., 1993; Strauss et al., 1997). The slowly continuing phosphate immobilization over weeks by goethite has been verified to be due to diffusion of phosphate into micropores (Strauss et al., 1997). Similarly, a clogging of micropores of drinking-water treatment residuals that comprise amorphous hydrous Fe and Al oxides by phosphate has recently been confirmed (Makris et al., 2004). The micropore diffusion of phosphate in our study is further evidenced by decreasing average micropore diameters when phosphate was added to pure and C-coated goethite (Table 2). It is important to note, however, that the high-surface-area goethite used partially recrystallized in solution. This is shown by the decrease in the micropore volume and a

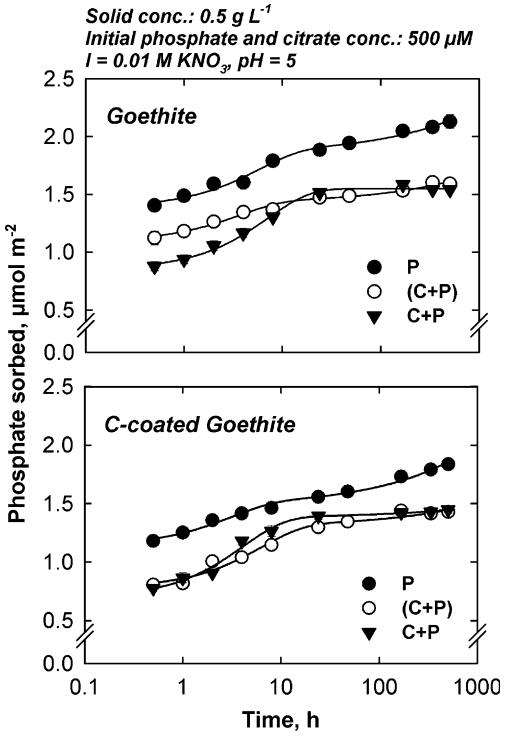

Fig. 2. Phosphate sorption versus time of pure goethite and C-coated goethite. The lines show the fits of Eq. (1) to the phosphate sorption data. Treatments: P, phosphate addition; (C + P), simultaneous addition of citrate and phosphate; C + P, citrate added 3 h before phosphate. Number of replicates was 3; subsample variability was <2% on average. Error bars representing the standard deviation are within the symbol size.

Table 2
Specific surface area and porosity after 3 weeks of sorption of phosphate, citrate, or both ions using differing addition modes

Treatment	Specific surface area ($m^2\ g^{-1}$)	Total pore volume ($mm^3\ g^{-1}$)	Average pore diameter (nm)	Mesopore volume ($mm^3 g^{-1}$)			Micropore volume ($mm^3\ g^{-1}$)	Average micropore diameter (nm)
				2–5 nm	5–10 nm	10–50 nm		
Goethite								
Initial[a]	178.8 (5.9)	647 (15)	14.5 (0.2)	75 (6)	89 (3)	420 (12)	57 (1)	0.87 (0.01)
No P	136.7 (1.6)a	538 (15)a	15.7 (0.4)a	45 (3)a	77 (1)a	346 (2)a	41 (0)a	0.91 (0.01)a
P	151.1 (1.3)bc	540 (9)a	14.3 (0.1)b	45 (3)a	79 (1)a	358 (4)b	44 (1)b	0.75 (0.02)b
(C + P)	155.5 (2.0)b	529 (3)a	13.6 (0.1)c	48 (4)a	84 (1)b	354 (5)a	40 (0)c	0.71 (0.00)c
C + P	150.7 (1.6)c	565 (20)a	15.0 (0.7)ab	47 (2)a	77 (2)a	364 (12)a	39 (0)d	0.72 (0.01)bc
Goethite/DOM								
Initial[a]	149.3 (4.2)	620 (7)	16.6 (0.3)	53 (5)	76 (2)	417 (9)	44 (0)	0.87 (0.01)
No P	135.8 (0.9)a	581 (2)a	17.1 (0.1)a	41 (0)a	74 (1)a	367 (1)a	38 (0)a	0.90 (0.01)a
P	149.9 (1.7)bc	579 (6)a	15.5 (0.1)b	45 (3)a	80 (2)b	370 (4)a	40 (0)b	0.73 (0.01)b
(C + P)	153.6 (1.9)b	566 (13)a	14.7 (0.2)c	53 (5)b	80 (2)b	354 (6)b	39 (0)b	0.73 (0.01)b
C + P	146.2 (4.0)c	574 (9)a	15.7 (0.2)b	43 (3)a	76 (4)ab	368 (9)ab	38 (1)a	0.74 (0.03)b

Treatments: Goethite-initial and Goethite/DOM-initial, goethite properties at the beginning of the sorption experiments, i.e., no solution contact; no P, samples in background electrolyte (control); P, phosphate addition; (C + P), simultaneous addition of citrate and phosphate; C + P, citrate added 3 h before phosphate. Means were compared using the unpaired *t*-test. For each adsorbent, values in the same column that are followed by the same letter are not statistically different at $P < 0.05$. Values in parentheses represent standard deviation.
[a] Initial, no solution contact.

concomitant increase in the average micropore diameter after 3 weeks compared with the initial goethite (Table 2). Accordingly, the healing of the smallest surface inhomogeneities (micropores) increased the average micropore diameter as well as decreased the micropore volume. The strongly complexing phosphate counteracted the goethite transformation to some extent, which resulted in greater micropore volumes of phosphate-treated samples relative to the controls (no P, Table 2). This inhibitory effect of specifically sorbing ligands like phosphate has also been shown to retard ferrihydrite transformation (Barrón et al., 1997). Despite the dynamic nature of the goethite surface, it can be unambiguously concluded that phosphate penetrated into micropores as their average diameters decreased during 3 weeks with respect to the initial goethite's average micropore diameter (Table 2).

While the sorption of phosphate to external surfaces was reduced by 21% due to the DOM coating (Table 3, c_m), the slowly sorbing phosphate fraction, P_{slowly}, and the apparent diffusion constant $(D/r^2)_{app}$ were not significantly affected (Table 3). Therefore, the diffusion of phosphate into micropores of goethite was likely not restricted by DOM as shown by a similar decrease in average micropore diameter compared with pure goethite (Table 2). It is particularly noteworthy that the ζ-potential of goethite was reversed upon DOM sorption from +29 to −32 mV and remained negative upon phosphate sorption (Fig. 3B) and that only 43% of C were desorbed from C-coated goethite upon phosphate sorption within 3 weeks. Consequently, the phosphate diffusion into micropores of C-coated goethite was hardly influenced by the decreased ζ-potential caused by sorbed DOM molecules. The phosphate sorption kinetics of C-coated goethite is clearly inconsistent with the preferential sorption and stabilization of organic matter in pores <10 nm (Kaiser and Guggenberger, 2003; Zimmerman et al., 2004a). The proposed

Table 3
Parameter obtained from fitting the combined model to the phosphate sorption data, apparent diffusion constant $(D/r^2)_{app}$ and the amount of phosphate slowly immobilized during 3 weeks

Treatment	c_m[a] (μmol m^{-2})	a_0[b] (μmol m^{-2})	k[c] (h^{-1})	b[d] (μmol $m^{-2}\ h^{-0.5} \times 10^{-3}$)	r^2	$(D/r^2)_{app}$ ($h^{-1} \times 10^{-7}$)	$P_{slowly,}\ q_{504h} - c_m$ (μmol m^{-2})
Goethite							
P	1.85 (0.04)	0.46 (0.04)	0.18 (0.04)	13 (2)	0.99	23.7 (8.8)	0.29 (0.05)
(C + P)	1.42 (0.02)	0.33 (0.03)	0.29 (0.07)	9 (2)	0.98	8.4 (3.1)	0.17 (0.02)
C + P	1.55 (0.04)	0.70 (0.04)	0.14 (0.02)	NS	0.99	NS	0.00 (0.04)
Goethite/DOM							
P	1.47 (0.02)	0.34 (0.04)	0.36 (0.10)	17 (2)	0.99	34.7 (6.8)	0.36 (0.03)
(C + P)	1.30 (0.05)	0.52 (0.06)	0.16 (0.04)	7 (3)	0.98	4.8 (4.7)	0.13 (0.05)
C + P	1.38 (0.04)	0.69 (0.05)	0.25 (0.05)	NS	0.99	NS	0.07 (0.05)

Treatments: P, phosphate addition; (C + P), simultaneous addition of citrate and phosphate; C + P, citrate added 3 h before phosphate. Values in parentheses represent standard error.
[a] Total amount of phosphate sorbed rapidly.
[b] Constant related to the amount of phosphate instantaneously sorbed according to Eq. (2).
[c] Rate constant of the fast phosphate reaction.
[d] Rate constant of the slow phosphate reaction. NS indicates nonsignificance at the $P = 0.10$ level.

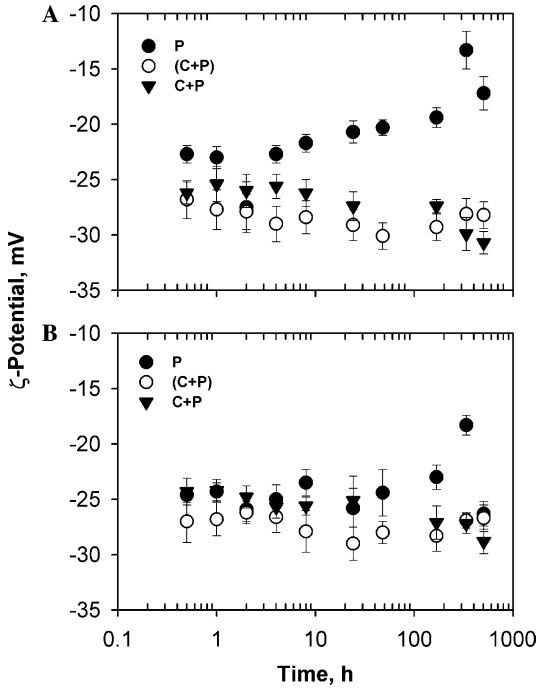

Fig. 3. Change of ζ-potential with time of (A) pure goethite and (B) C-coated. Treatments: P, phosphate addition; (C + P), simultaneous addition of citrate and phosphate; C + P, citrate added 3 h before phosphate. Error bars represent standard deviation. The initial ζ-potential of pure and C-coated goethite in 0.01 M KNO_3 (pH 5) was +29 and −32 mV, respectively.

preferential sorption of DOM molecules in or at the mouths of micropores (Kaiser and Guggenberger, 2003) should render these organic molecules less desorbable by phosphate, and – more important – should decrease the accessibility of these pores to phosphate ions. Therefore, the observed inconsistency between the strong reduction in pore volume of pores <10 nm in C-coated goethite samples (Table 1) and both a similar slow phosphate sorption kinetics and change in average micropore diameter after phosphate sorption compared with pure goethite (Tables 2 and 3) might be best explained by structural changes of DOM-molecules at the goethite surface upon drying. Drying of organic coatings might decrease the accessibility of pores <10 nm for N_2 at 77 K. In a previous study, Mikutta et al. (2004) showed that mesopore volumes of a hydrous Al oxide sample coated with polygalacturonate decreased upon drying.

3.3. Citrate-promoted goethite dissolution during phosphate sorption

Iron concentrations in solution increased linearly in the presence of citrate, and up to 2.3 mol% Fe of pure and C-coated goethite were dissolved within 3 weeks (Fig. 4). The zero-order dissolution kinetics of goethite complies with a surface-controlled, ligand-promoted dissolution that has been described by Stumm and coworkers (Furrer and Stumm, 1986; Zinder et al., 1986; Stumm and Furrer, 1987). This effect was greater for C-coated goethite and samples to which citrate was added before phosphate

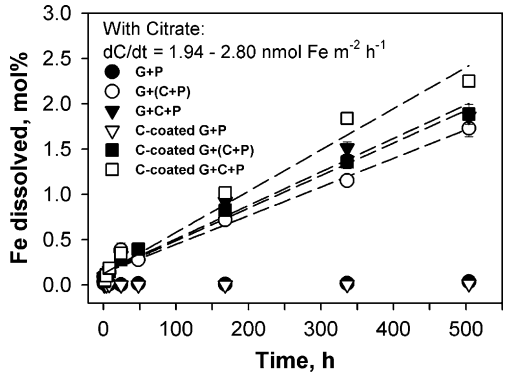

Fig. 4. Iron release kinetics of pure (G) and C-coated goethite (C-coated G) in the presence of citrate following different modes of addition ($I = 0.01$ M, pH 5). The solid lines were obtained by linear curve fitting. Coefficients of determination were ⩾0.98. Treatments: P, phosphate addition; (C + P), simultaneous addition of citrate and phosphate; C + P, citrate added 3 h before phosphate. Error bars representing standard deviation are smaller than the symbol size. The Fe release rates of pure and C-coated goethite were normalized to the N_2-BET surface area of pure goethite (179 $m^2\ g^{-1}$).

(Fig. 4). Dissolution of pure and C-coated goethite proceeded at higher rates at times <∼24 h. The initial fast dissolution was followed by a slower linear dissolution pattern; a finding that was also reported for lepidocrocite (Bondietti et al., 1993) and hematite (Sulzberger et al., 1989). The initial fast dissolution is attributed to the rapid dissolution of surface irregularities of crystals or to the dissolution of small particles (Ostwald ripening), like for instance, ferrihydrite particles in goethite/ferrihydrite mixtures (Schwertmann et al., 1982). The initial fast dissolution step was small compared with the linear dissolution pattern in our and related studies on crystalline Fe oxides (Sulzberger et al., 1989; Bondietti et al., 1993), but became the controlling process in the citrate-mediated dissolution of ferrihydrite (Liang et al., 2000).

If the Fe dissolved rapidly is attributed to residual ferrihydrite, the contribution of dissolved residual ferrihydrite to the sample's mass would be 0.44 wt% in the treatment with maximal Fe release (C-coated goethite, 'C-coated G + C + P' in Fig. 4). This value corresponds to a maximal ferrihydrite contribution of <1 $m^2\ g^{-1}$ to the total N_2-BET surface area – a value, which cannot be resolved by N_2 surface area measurements. As changes in micropore surface area were larger than 1 $m^2\ g^{-1}$ in the presence of citrate, microporosity data discussed hereafter are likely not biased by the presence of residual ferrihydrite.

Sorption of citrate before phosphate to pure goethite decreased the ability of phosphate to compete with citrate for sorption sites (Table 4). In accordance with the ligand-promoted, nonreductive dissolution of hydrous Fe oxides by organic ligands, R_L, that is linearly dependent on the concentration of the adsorbed ligand (L_{ads}):

$$R_L = d[Fe(III)_{aq}]/dt = k_L[L_{ads}], \quad (6)$$

where k_L is the rate constant of ligand-promoted dissolution (Stumm, 1992), higher adsorption densities of citrate

Table 4
Amounts of phosphate and citrate sorbed after 1 and 24 h

Treatment	Sorption after 1 h (μmol m^{-2})			Sorption after 24 h (μmol m^{-2})		
	P	Citrate	Σ(P + Citrate)	P	Citrate	Σ(P + Citrate)
Goethite						
P	1.49 (0.03)		1.49 (0.03)	1.88 (0.02)		1.88 (0.02)
(C + P)	1.18 (0.05)	0.30 (0.10)	1.48 (0.11)	1.48 (0.01)	0.16 (0.00)	1.64 (0.01)
C + P	0.94 (0.04)	0.69 (0.05)	1.62 (0.06)	1.51 (0.02)	0.62 (0.07)	2.13 (0.08)
Goethite/DOM						
P	1.25 (0.02)		1.25 (0.02)	1.56 (0.02)		1.56 (0.02)
(C + P)	0.82 (0.01)	0.30 (0.03)	1.12 (0.03)	1.30 (0.04)	0.27 (0.01)	1.57 (0.04)
C + P	0.86 (0.04)	0.40 (0.04)	1.26 (0.06)	1.40 (0.03)	0.25 (0.02)	1.65 (0.04)

Treatments: P, phosphate addition; (C + P), simultaneous addition of citrate and phosphate; C + P, citrate added 3 h before phosphate. Values in parentheses represent standard deviation.

in the 'C + P' treatment (Table 4) facilitated the partial dissolution of pure goethite. As a consequence, higher Fe concentrations were measured in solution in the 'C + P' treatment (Fig. 4). When both ions were added simultaneously, citrate sorption was strongly reduced (Table 4) and the dissolution of goethite was less distinct (Fig. 4). Our results are in line with Watanabe and Matsumoto (1994) and Hiradate and Inoue (1998) who observed that the dissolution of Fe oxides by mugineic acid was inhibited by phosphate due to sorption competition. The effect of the order of addition of both ions on P_{slowly} of C-coated goethite was less evident compared with pure goethite (Table 3). While the amount of citrate sorbed to C-coated goethite after 1, 24 (Table 4) and 504 h (not shown) was similar in both citrate treatments, TOC concentrations in solution were 23% higher in the 'C + P' treatment compared to the '(C + P)' treatment after 3 weeks. Likewise, Fe concentrations in solution after 3 weeks were 19% higher when citrate was added before phosphate to C-coated goethite (Fig. 4). These findings indicate that either citrate alone or in combination with phosphate promoted the partial dissolution of C-coated goethite by favoring the release of Fe(III)–organic matter complexes from the goethite surface. A similar synergistic effect of LMWOA anions on the ligand-promoted dissolution of goethite has been reported for oxalate, which enhanced the rate of goethite dissolution by the fungal siderophore desferrioxamine B (Cervini-Silva and Sposito, 2002; Cheah et al., 2003).

3.4. Phosphate sorption kinetics in the presence of citrate

Phosphate sorption induced the desorption of citrate from pure and C-coated goethite (Table 4). Despite the strong competition between both ions, citrate decreased the amount of phosphate sorbed to pure and C-coated goethites after 3 weeks by up to 28% and 22%, respectively. The result complies with Geelhoed et al. (1998) who reported a pronounced decrease in phosphate sorption at pH 5 when citrate was present at equimolar concentration.

The effect of citrate on the phosphate sorption kinetics of goethite can be slit up into two separate processes: First, citrate reduced the amount of phosphate sorbed to external surfaces of both adsorbents (Table 3, c_m), which can be attributed to direct site blocking. Second, citrate reduced the amount of phosphate sorbed to internal sorption sites (Table 3, P_{slowly}). The latter effect of citrate was more pronounced compared with the sorption competition between phosphate and citrate for external surface sites.

The rate constant of the slow phosphate immobilization, b, decreased for pure and C-coated goethite in the order P > (C + P) ≫ C + P (Table 3). The amount of phosphate diffused, approximated as P_{slowly}, decreased for pure goethite in the order P > (C + P) ≫ C + P, but no statistically significant effect of the order of addition on the slow phosphate immobilization could be found for C-coated goethite (P > (C + P) = C + P; Table 3). Apparent diffusion constants, $(D/r^2)_{app}$, reported in Table 3 comply well with apparent diffusion constants reported for molybdenum desorption from pure and C-coated goethites (Lang and Kaupenjohann, 2003), but are 3–4 orders of magnitude lower than those reported for phosphate sorption to goethites (Strauss et al., 1997), which may be caused by a systematic overestimation of q_∞ as an approximation for the amount of phosphate diffused at infinite time in Eq. (2). Apparent diffusion constants decreased in the presence of citrate and became statistically insignificant at $P = 0.10$ when citrate was added before phosphate (Table 3). This finding indicates that the diffusion resistance of phosphate increased in the citrate treatments as a consequence of the micropore volume and micropore diameter reduction (Table 2). The stronger the reduction in micropore volume was for pure goethite, i.e., C + P ≫ (C + P), the less phosphate was slowly immobilized during 3 weeks (Fig. 5).

We observed an inverse relationship between the amount of Fe dissolved (μmol g^{-1}) after 3 weeks and the specific micropore volume still present after 3 weeks ($n = 5$, $r^2 = 0.97$, $P = 0.003$). The treatment 'C-coated goethite + P' had to be excluded from the regression analysis, because the Fe release in this treatment was possibly impaired by sorbed DOM thus producing an outlier in the data. Despite that, the observed relationship implies that in the presence of citrate both the clogging of micropores

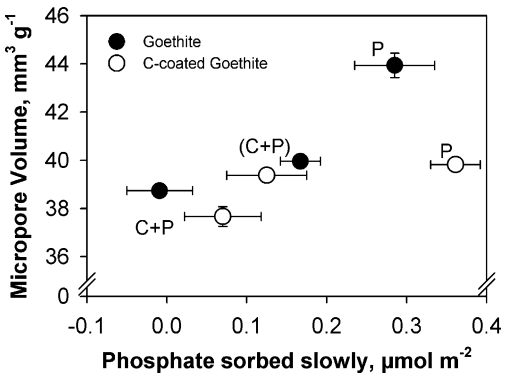

Fig. 5. Phosphate sorbed slowly calculated according to Eq. (3) versus the micropore volume present after 3 weeks of sorption. Treatments: P, phosphate addition; (C + P), simultaneous addition of citrate and phosphate; C + P, citrate added 3 h before phosphate. Error bars indicate standard error.

as shown in the short-term citrate sorption experiment (Table 1) and the partial dissolution of goethite proceeding at external goethite surfaces may account for (i) the reduction in micropore volume and average micropore diameter (Table 2), and hence (ii) the reduction in the rate constant of the slow phosphate sorption and the amount of slowly sorbing phosphate (Table 3). Based on our results, we cannot discern which of the two processes leading to a reduced microporosity prevailed.

3.5. Electrophoretic mobility measurements

The ζ-potential kinetics are presented in Fig. 3. Phosphate sorption to pure goethite reversed its ζ-potential to negative values, which accords with the finding that specifically sorbing anions lead to a reversal of the ζ-potential with increasing ion concentration (Hunter, 1981; Goldberg et al., 1996; Su and Suarez, 2000). With increasing sorption time, the ζ-potential of pure goethite increased by about 6 mV during phosphate sorption, which was not noticeable for C-coated goethite (Fig. 3). Possible explanations include surface precipitation of Fe phosphates (Ler and Standforth, 2003; Kim and Kirkpatrick, 2004), disaggregation of goethite particles (Lima et al., 2000), or diffusion of phosphate into pores of the adsorbent (Strauss et al., 1997; Makris et al., 2004), where it does no more contribute to the electrophoretic mobility. We favor the latter explanation because (i) phosphate clogged micropores of pure goethite and C-coated goethite in the absence of citrate (Table 4, average micropore diameter), (ii) no surface precipitation of phosphate on goethite could be detected by XANES over a broad range of phosphate concentrations in solution (0–1.4 mM) (Khare et al., 2005), and (iii) the Fe release kinetics were not related to the ζ-potential kinetics (Figs. 3 and 4).

In the presence of citrate the ζ-potential of the adsorbents declined when compared with samples to which only phosphate was added, showing that citrate conveyed additional negative charge to the adsorbents surface (Fig. 3). This effect was stronger for pure goethite compared with C-coated goethite. The order of addition of both ions to pure goethite did not result in significant differences in the ζ-potential, which accords with the minor effect of the order of addition on the amount of phosphate sorbed to external surfaces (Table 3, c_m). This result indicates that externally sorbed ions contribute primarily to the electrophoretic mobility.

4. Environmental implications

Polyprotic low-molecular-weight organic acid anions are excreted by plant roots at rates ranging up to 4000 nmol g^{-1} (fresh weight) h^{-1} depending on environmental conditions (Ryan et al., 2001). Consequently, concentrations of these anions in rhizosphere soil solution can increase up to 1500 µM (Jones, 1998). Modeling approaches indicate that 99% of these acids remain within 1 mm from the root surface (Jones et al., 1996), which confines their efficiency in nutrient acquisition to the soil–root interface. Phosphate mobilization mediated by LMWOA anions has been documented for soils (e.g., Lopez-Hernandez et al., 1986; Traina et al., 1987; Jungk et al., 1993; Strom et al., 2002), but the mechanisms behind are not easily identifiable in complex systems. The increase in phosphate solution concentration in the presence of LMWOA anions has mostly been ascribed to sorption competition (Lopez-Hernandez et al., 1986; Geelhoed et al., 1998, 1999; see Guppy et al., 2005 for a review) and, less often, to the dissolution of phosphate-bearing minerals (Traina et al., 1987; Bolan et al., 1994, 1997; Bertrand et al., 1999). Although the dissolution of hydrous Fe oxides by LMWOA anions is well documented (Stumm et al., 1985; Miller et al., 1986; Zinder et al., 1986; Chiarizia and Horwitz, 1991), its ecological meaning has received much less attention (Jones et al., 1996; Bertrand and Hinsinger, 2000).

In accordance with adsorption studies (e.g., Geelhoed et al., 1998), sorption competition between citrate and phosphate decreased the sorption of phosphate to pure and C-goethite by up to 28%. Additionally, citrate clogged the micropores of goethite and enhanced the adsorbent's dissolution—two mechanisms by which the diffusion of phosphate into mineral pores of <2-nm size and hence its strong fixation can be reduced.

The sorption of citrate in micropores of pure and C-coated goethites was detectable within the maximal average half-live time reported for citrate in soils (<12 h, Jones and Darrah, 1994) without any significant dissolution of the goethite occurring (<0.3 mol% Fe). The sorption of citrate in micropores of goethite within hours may partially promote its stabilization against microbial decay by the physical exclusion of enzymes (Adu and Oades, 1978; Mayer, 1994; Zimmerman et al., 2004a,b). Within 3 weeks of phosphate sorption to pure and C-coated goethite, citrate significantly impaired the slow phosphate reaction. Both micropore clogging by citrate and/or citrate-mediated goethite dissolution (<2.3 mol% Fe) were identified as possible

mechanisms by which the diffusion of phosphate into micropores of pure and C-coated goethites can be impaired. As plants under phosphate stress will exude LMWOA anions at high rates and over long periods of time, the micropore clogging or the dissolution of strongly phosphate sorbing hydrous Fe and Al oxides adjacent to root surfaces may be regarded as potential strategies of plants to cope with phosphate deficiency in addition to ligand-exchange. The effects of micropore clogging by LMWOA anions and the dissolution of hydrous Fe oxides by polyprotic LMWOA anions on the phytoavailability of phosphate have yet not been realized, and are therefore still unaccounted for in mathematical models of phosphate mobilization by organic anion excretion by plant roots (Geelhoed et al., 1999; Kirk, 1999).

5. Conclusions

Under the experimental conditions chosen, citrate as a common water-soluble root exudate has been shown to clog the micropores of both a synthetic pure goethite and one that was coated with dissolved organic matter. For both adsorbents, the micropore clogging proceeded within only a few hours. The micropore clogging of both adsorbents by citrate increased with time and, for C-coated goethite, with increasing citrate concentration.

During 3 weeks of phosphate sorption in the presence of citrate at equimolar concentration (500 μM), citrate reduced the amount of phosphate sorbed to both adsorbents by up to 28%, and solubilized Fe from pure and C-coated goethite by up to 2.3 mol%. In addition, citrate led to a reduction in the micropore volume and average micropore diameter of pure and C-coated goethite. Consequently, the slow and continuous phosphate immobilization by both adsorbents via diffusion of phosphate into micropores was strongly impaired. This effect was larger when citrate was added 3 h before phosphate to pure goethite, but only a minor effect of the order of addition of both ions was observed for C-coated goethite. As both microporous hydrous Fe oxides and LMWOA anions are ubiquitous in soils and sediments, micropore-clogging and/or the partial dissolution of hydrous Fe oxides by LMWOA anions might be of significant importance regarding the mobility of nutrient and/or contaminant anions that would otherwise be strongly fixed by hydrous Fe oxides in acidic environments.

Due to phase transformations of meta-stable microporous adsorbents in aqueous solutions, the *average micropore diameter* can be regarded as a better parameter for identifying micropore clogging or dissolution reactions caused by organic compounds than simply *micropore volume*.

Acknowledgments

We thank Klaus Kaiser (Martin-Luther University Halle-Wittenberg) for his help with the synthesis of the goethite, Robert Mikutta (Martin-Luther University Halle-Wittenberg) for the X-ray diffraction analysis, and Peter Dominik for the differential X-ray diffraction analysis. We appreciated the support of three anonymous reviewers who helped to improve the manuscript. This research was funded by the German Research Fund (DFG, KA 1139/8).

Associated editor: Garrison Sposito

References

Adu, J.K., Oades, J.M., 1978. Physical factors influencing decomposition of organic materials in soil aggregates. *Soil Biol. Biochem.* **10**, 109–115.

Anderson, M.A., Tejedor-Tejedor, M.I., Stanforth, R.R., 1985. Influence of aggregation on the uptake kinetics of phosphate by goethite. *Environ. Sci. Technol.* **19**, 632–637.

Barrett, E.P., Joyner, L.G., Halenda, P.P., 1951. The determination of pore volume and area distributions in porous substances. I. Computations from nitrogen isotherms. *J. Am. Chem. Soc.* **73**, 373–380.

Barrón, V., Gálvez, N., Hochella Jr., M.F., Torrent, J., 1997. Epitaxial overgrowth of goethite on hematite synthesized in phosphate media: a scanning force and transmission electron microscopy study. *Am. Mineral.* **82**, 1091–1100.

Barrow, N.J., Madrid, L., Posner, A.M., 1981. A partial model for the rate of adsorption and desorption of phosphate by goethite. *J. Soil Sci.* **32**, 399–407.

Barrow, N.J., Brümmer, G.W., Strauss, R., 1993. Effects of surface heterogeneity on ion adsorption by metal oxides and by soils. *Langmuir* **9**, 2606–2611.

Bertrand, I., Hinsinger, P., 2000. Dissolution of iron oxyhydroxide in the rhizosphere of various crop species. *J. Plant Nutr.* **23**, 1559–1577.

Bertrand, I., Hinsinger, P., Jaillard, B., Arvieu, J.C., 1999. Dynamics of phosphorus in the rhizosphere of maize and rape grown on synthetic, phosphated calcite and goethite. *Plant Soil* **211**, 111–119.

Bhatti, J.S., Comerford, N.B., Johnston, C.T., 1998. Influence of oxalate and soil organic matter on sorption and desorption of phosphate onto a spodic horizon. *Soil Sci. Soc. Am. J.* **62**, 1089–1095.

Blakemore, L.C., Searle, P.L., Daly, B.K., 1987. Methods for chemical analysis of soils. NZ Soil Bureau Scientific Report 80, NZ Soil Bureau, Lower Hutt.

Bolan, N.S., Naidu, R., Mahimairaja, S., Baskaran, S., 1994. Influence of low-molecular-weight organic acids on the solubilization of phosphates. *Biol. Fertil. Soils* **18**, 311–319.

Bolan, N.S., Elliot, J., Gregg, P.E.H., Weil, S., 1997. Enhanced dissolution of phosphate rocks in the rhizosphere. *Biol. Fertil. Soils* **24**, 169–174.

Bondietti, G., Sinniger, J., Stumm, W., 1993. The reactivity of Fe(III) (hydr)oxides: effects of ligands in inhibiting the dissolution. *Colloid Surf. A.* **79**, 157–167.

Borggaard, O.K., 1988. Phase identification by selective dissolution techniques. In: Stucki, J.W., Goodman, B.A., Schwertmann, U. (Eds.), *Iron in Soils and Clay Minerals*. Reidel, Dordrecht, pp. 83–98.

Borggaard, O.K., 1990. Kinetics and mechanism of soil iron oxide dissolution in EDTA, oxalate, and dithionite. *Sci. Geol. Mem.* **85**, 139–148.

Brunauer, S., Emmett, P.H., Teller, E., 1938. Adsorption of gases in multimolecular layers. *J. Am. Chem. Soc.* **60**, 309–319.

Cervini-Silva, J., Sposito, G., 2002. Steady-state dissolution kinetics of aluminum-goethite in the presence of desferrioxamine-B and oxalate ligands. *Environ. Sci. Technol.* **36**, 337–342.

Cheah, S.F., Kraemer, S.M., Cervini-Silva, J., Sposito, G., 2003. Steady-state dissolution kinetics of goethite in the presence of desferrioxamine B and oxalate ligands: implications for the microbial acquisition of iron. *Chem. Geol.* **198**, 63–75.

Chiarizia, R., Horwitz, E.P., 1991. New formulations for iron oxides dissolution. *Hydrometallurgy* **27**, 339–360.

Cornell, R.M., Schindler, P.W., 1980. Infrared study of the adsorption of hydroxycarboxylic acids on α-FeOOH and amorphous Fe(III)-hydroxide. *Colloid Polymer Sci.* **258**, 1171–1175.

Cornell, R.M., Schwertmann, U., 2003. *The Iron Oxides. Structure, Properties, Reactions, Occurrences and Uses*, second ed. Wiley-VCH, Weinheim.

Crank, J., 1976. *The Mathematics of Diffusion*. Oxford University Press, New York.

Edwards, A.P., Bremmer, J.M., 1967. Microaggregates in soils. *J. Soil Sci.* **18**, 64–73.

Fine, P., Singer, M.J., 1989. Contribution of ferrimagnetic minerals to oxalate-and dithionite extractable iron. *J. Soil Sci. Soc. Am.* **53**, 191–196.

Fischer, L., zur Mühlen, E., Brümmer, G.W., Niehus, E., 1996. Atomic force microscopy (AFM) investigations of the surface topography of a multidomain porous goethite. *Eur. J. Soil Sci.* **47**, 329–334.

Fuller, C.C., Davis, J.A., Waychunas, G.A., 1993. Surface chemistry of ferrihydrite: Part 2. Kinetics of arsenate adsorption and coprecipitation. *Geochim. Cosmochim. Acta* **57**, 2271–2282.

Furrer, G., Stumm, W., 1986. The coordination chemistry of weathering . I. Dissolution kinetics of γ-Al_2O_3 and BeO. *Geochim. Cosmochim. Acta* **50**, 1847–1860.

Geelhoed, J.S., Hiemstra, T., Van Riemsdijk, W.H., 1998. Competitive interaction between phosphate and citrate on goethite. *Environ. Sci. Technol.* **32**, 2119–2123.

Geelhoed, J.S., Van Riemsdijk, W.H., Findenegg, G.R., 1999. Simulation of the effect of citrate exudation from roots on the plant availability of phosphate adsorbed on goethite. *Eur. J. Soil Sci.* **50**, 379–390.

Gerin, P.A., Genet, M.J., Herbillon, A.J., Delvaux, B., 2003. Surface analysis of soil material by X-ray photoelectron spectroscopy. *Eur. J. Soil Sci.* **54**, 589–603.

Goldberg, S., Forster, H.S., Godfrey, C.L., 1996. Molybdenum adsorption of oxides, clay minerals, and soils. *Soil Sci. Soc. Am. J.* **60**, 425–432.

Gregg, S.J., Sing, K.S.W., 1982. *Adsorption, Surface Area and Porosity*, second ed. Academic Press, New York.

Guppy, C.N., Menzies, N.W., Moody, P.W., Blamey, F.P.C., 2005. Competitive sorption reactions between phosphorus and organic matter in soil: a review. *Austr. J. Soil Res.* **43**, 189–202.

Hiradate, S., Inoue, K., 1998. Interaction of mugineic acid with iron (hydr)oxides: sulfate and phosphate influences. *Soil Sci. Soc. Am. J.* **62**, 159–165.

Hu, H.Q., He, J.Z., Li, X.Y., Liu, F., 2001. Effect of several organic acids on phosphate adsorption by variable charge soils of Central China. *Environ. Int.* **26**, 353–358.

Hue, N.V., 1991. Effects of organic acids/anions on P sorption and phytoavailability in soils with different mineralogy. *Soil Sci.* **6**, 463–471.

Hunter, R.J., 1981. *Zeta Potential in Colloid Science, Principles and Applications*. Academic Press, London.

Jones, D.L., 1998. Organic acids in the rhizosphere – a critical review. *Plant Soil* **205**, 25–44.

Jones, D.L., Darrah, P.R., 1994. Role of root derived organic acids in the mobilisation of nutrients from the rhizosphere. *Plant Soil* **166**, 247–257.

Jones, D.L., Darrah, P.R., Kochian, L.V., 1996. Critical-evaluation of organic-acid mediated iron dissolution in the rhizosphere and its potential role in root iron uptake. *Plant Soil* **180**, 57–66.

Jungk, A., Seeling, B., Gerke, J., 1993. Mobilization of different phosphate fractions in the rhizosphere. *Plant Soil* **155/156**, 91–94.

Kaiser, K., Guggenberger, G., 2003. Mineral surface and soil organic matter. *Eur. J. Soil Sci.* **54**, 219–236.

Khare, N., Hesterberg, D., Martin, J.D., 2005. XANES investigation of phosphate sorption in single and binary systems of iron and aluminum oxide minerals. *Environ. Sci. Technol.* **39**, 2152–2160.

Kim, Y., Kirkpatrick, R.J., 2004. An investigation of phosphate adsorbed on aluminium oxyhydroxide and oxide phases by nuclear magnetic resonance. *Eur. J. Soil Sci.* **55**, 243–251.

Kirk, G.J.D., 1999. A model of phosphate solubilization by organic anion excretion from plant roots. *Eur. J. Soil Sci.* **50**, 369–378.

Lang, F., Kaupenjohann, M., 2003. Immobilisation of molybdate by iron oxides: effect of organic coatings. *Geoderma* **113**, 31–46.

Ler, A., Standforth, R., 2003. Evidence of surface precipitation pf phosphate on goethite. *Environ. Sci. Technol.* **37**, 2694–2700.

Liang, L., Hofmann, A., Gu, B., 2000. Ligand-induced dissolution and release of ferrihydrite colloids. *Geochim. Cosmochim. Acta* **64**, 2027–2037.

Lima, J.M., Anderson, S.J., Curi, N., 2000. Phosphate-induced clay dispersion as related to aggregate size and composition in Hapludoxs. *Soil Sci. Soc. Am. J.* **64**, 892–897.

Lopez-Hernandez, D., Siegert, G., Rodriguez, J.V., 1986. Competitive adsorption of phosphate with malate and oxalate by tropical soils. *Soil Sci. Soc. Am. J.* **50**, 1460–1462.

Makris, K.C., Harris, W.G., O'Connor, G.A., Obreza, T.A., 2004. Phosphorus immobilization in micropores of drinking-water treatment residuals: implications for long-term stability. *Environ. Sci. Technol.* **38**, 6590–6596.

Mayer, L.M., 1994. Relationships between mineral surfaces and organic carbon concentrations in soils and sediments. *Chem. Geol.* **114**, 347–363.

Mayer, L.M., 1999. Extend of coverage of mineral surfaces by organic matter in marine sediments. *Geochim. Cosmochim. Acta* **63**, 207–215.

Mayer, L.M., Xing, B., 2001. Organic matter-surface area relationships in acid soils. *Soil Sci. Soc. Am. J.* **65**, 250–258.

McKeague, J.A., Brydon, J.E., Miles, N.M., 1971. Differentiation of forms of extractable iron and aluminum in soils. *Proc. Soil Sci. Soc. Am.* **35**, 33–38.

Mikutta, C., Lang, F., Kaupenjohann, M., 2004. Soil organic matter clogs mineral pores: evidence from ^{1}H-NMR logging and N_2 adsorption. *Soil Sci. Soc. Am. J.* **68**, 1853–1862.

Mikutta, C., Lang, F., Kaupenjohann, M., 2006. Kinetics of phosphate sorption to polygalacturonate-coated goethite. *Soil Sci. Soc. Am. J.* (in press).

Miller, W.P., Zelazny, L.W., Martens, D.C., 1986. Dissolution of synthetic crystalline and noncrystalline iron oxides by organic acids. *Geoderma* **37**, 1–13.

Möllering, H., Gruber, W., 1966. Determination of citrate with citrate lyase. *Anal. Biochem.* **17**, 369–376.

Murphy, J., Riley, J.P., 1962. A modified single solution method for determination of phosphate in natural waters. *Anal. Chim. Acta* **26**, 31–36.

Nordman, C.E., Weldon, A.S., Patterson, A.L., 1960. X-ray crystal analysis of the substrates of aconitase. II. Anhydrous citric acid. *Acta Crystallogr.* **13**, 418–426.

Olson, R.V., Ellis, R., 1982. Iron. In: Page, A.L. (Ed.), *Methods of Soil Analysis, Part 2, Chemical and Microbiological Properties. Agronomy Monograph No. 9*. American Society of Agronomy-Soil Science Society of America, Madison, WI, pp. 301–312.

Pinheiro-Dick, D., Schwertmann, U., 1996. Microaggregates from Oxisols and Inceptisols: dispersion through selective dissolutions and physicochemical treatments. *Geoderma* **74**, 49–63.

Ryan, P.R., Delhaize, E., Jones, D.L., 2001. Function and mechanism of organic anion exudation from plant roots. *Annu. Rev. Plant Physiol. Plant Mol. Biol.* **52**, 527–560.

Schwertmann, U., 1973. Use of oxalate for Fe extraction from soils. *Can. J. Soil Sci.* **53**, 244–246.

Schwertmann, U., Schulze, D.G., Murad, E., 1982. Identification of ferrihydrite in soils by dissolution kinetics, differential C-ray diffraction and Mössbauer spectroscopy. *Soil Sci. Soc. Am. J.* **46**, 869–875.

Strauss, R., 1992. Mechanismen der Phosphatbindung an Goethit. Phosphatadsorption und -diffusion in Abhängigkeit von der Goethitkristallinität. Bonner Bodenkundliche Abhandlung 5. Bonn, 284pp.

Strauss, R., Brümmer, G.W., Barrow, N.J., 1997. Effects of crystallinity of goethite: II. Rates of sorption and desorption of phosphate. *Eur. J. Soil Sci.* **48**, 101–114.

Strom, L., Owen, A.G., Godbold, D.L., Jones, D.L., 2002. Organic acid mediated P mobilisation in the rhizosphere and uptake by maize roots. *Soil Biol. Biochem.* **34**, 703–710.

Stumm, W., 1992. *Chemistry of the Solid–Water Interface*. Wiley, New York, 428pp.

Stumm, W., Furrer, G., 1987. The dissolution of oxides and aluminum silicates: examples of surface-coordination-controlled kinetics. In: Stumm, W. (Ed.), *Aquatic Surface Chemistry*. Wiley Interscience, New York, pp. 197–219.

Stumm, W., Furrer, G., Wieland, E., Zinder, B., 1985. The effects of complex-forming ligands on the dissolution of oxides and aluminosilicates. In: Drever, J.I. (Ed.), *The Chemistry of Weathering*. Reidel, Dordrecht, pp. 55–74.

Su, C., Suarez, D.L., 2000. Selenate and selenite sorption on iron oxides: a infrared and electrophoretic study. *Soil Sci. Soc. Am. J.* **64**, 101–111.

Sulzberger, B., Suter, D., Siffert, C., Banwart, S., Stumm, W., 1989. Dissolution of Fe(III) (hydr)oxides in natural waters: laboratory assessment on the kinetics controlled by surface coordination. *Mar. Chem.* **28**, 127–144.

Torrent, J., 1987. Rapid and slow phosphate sorption by Mediterranean soils: effect of iron oxides. *Soil Sci. Soc. Am. J.* **51**, 78–82.

Torrent, J., 1991. Activation energy of the slow reaction between phosphate and goethites of different morphology. *Aust. J. Soil Res.* **29**, 69–74.

Torrent, J., Barrón, V., Schwertmann, U., 1990. Phosphate adsorption and desorption by goethites differing in crystal morphology. *Soil Sci. Soc. Am. J.* **54**, 1007–1012.

Torrent, J., Schwertmann, U., Barrón, V., 1992. Fast and slow phosphate sorption by goethite-rich natural materials. *Clays Clay Miner.* **40**, 14–21.

Towe, K.M., Bradley, W.F., 1967. Mineralogical constitution of colloidal 'hydrous ferric oxides'. *J. Colloid Interf. Sci.* **24**, 384–392.

Traina, S.J., Sposito, G., Bradford, G.R., Kafkafi, U., 1987. Kinetic study of citrate effects on orthophosphate solubility in an acid, montmorillonitic soil. *Soil Sci. Soc. Am. J.* **51**, 1483–1487.

Violante, A., Colombo, C., Buondonno, A., 1991. Competitive adsorption of phosphate and oxalate by aluminum-oxides. *Soil Sci. Soc. Am. J.* **55**, 65–70.

Walker, A.L., 1983. The effects of magnetite on oxalate- and dithionite-extractable iron. *J. Soil Sci. Soc. Am.* **47**, 1022–1026.

Watanabe, S., Matsumoto, S., 1994. Effect of monosilicate, phosphate, and carbonate on iron dissolution by mugineic acid. *Soil Sci. Plant Nutr.* **40**, 9–17.

Willet, I.R., Chartres, C.J., Nguyen, T.T., 1988. Migration of phosphate into aggregated particles of ferrihydrite. *J. Soil Sci.* **39**, 275–282.

Zimmerman, A.R., Chorover, J., Goyne, K.W., Brantley, S.L., 2004a. Protection of mesopore-adsorbed organic matter from enzymatic degradation. *Environ. Sci. Technol.* **38**, 4542–4548.

Zimmerman, A.R., Goyne, K.W., Chorover, J., Komarneni, S., Brantley, S.L., 2004b. Mineral mesopore effect on nitrogenous organic matter adsorption. *Org. Geochem.* **35**, 355–375.

Zinder, B., Furrer, G., Stumm, W., 1986. The coordination chemistry of weathering. II. Dissolution of Fe(III) oxides. *Geochim. Cosmochim. Acta* **50**, 1861–1869.